

# Effect of force direction and tooth angulation during traction of palatally impacted canines: A finite element analysis

Kinan G. Zeno,<sup>a</sup> Samir Mustapha,<sup>b</sup> Georges Ayoub,<sup>c</sup> and Joseph G. Ghafari<sup>a,d</sup>  
Beirut, Lebanon, Dearborn, Mich, and Philadelphia, Pa

**Introduction:** Treatment of a palatally impacted canine (PIC) is associated with demanding anchorage control, increased treatment duration, and undesirable side effects. Accurate PIC localization and force application impact treatment success. The objective of this research was to determine the stresses on the PIC when subjected to initial force activation in various directions (buccal, vertical, and distal) and relative to impaction severity.

**Methods:** Thirty PICs from 21 scans underwent finite element modeling. A prototype 3D model was reconstructed and segmented into its anatomic components. Each PIC was precisely positioned in the prototype model according to impaction position. Stresses in response to a (1.0 N) force in the distal, vertical, and buccal directions were evaluated at different levels of the root (apical, middle, and cervical). **Results:** Distal and buccal forces yielded higher stress (6.64 and 6.41 kPa, respectively) than the vertical force (5.97 kPa) on the total PIC root and the apical and cervical root levels, but not at midroot. Statistically significant differences between severity groups were found mostly at the apical level among all force directions, except between distal and buccal forces in the higher severity group. In this group, stress was greatest at the cervical level with the buccal force significantly different from the stresses generated by either the distal or the vertical force. **Conclusions:** Vertical forces generated the lowest stresses. Differentially distributed stresses over the root reflected an initial tipping movement. Greater cervical stresses from the buccal force indicate resistance to movement, suggesting treatment initiation with vertical and distal forces over buccal forces, particularly with severely inclined canines. (Am J Orthod Dentofacial Orthop 2020;157:377-84)

Guidelines for the traction of a palatally impacted canine (PIC) depend on the accurate localization of the PIC<sup>1</sup> and the severity of its initial position.<sup>2</sup> Accordingly, orthodontic forces would be applied in the proper direction to avoid unwanted consequences

of tooth movement, such as longer treatment<sup>3-5</sup> and root resorption of the adjacent teeth, particularly the lateral incisor.<sup>6</sup>

Approaches to PIC traction varied from direct pull into the arch to the use of auxiliary springs supported by supplementary anchorage (transpalatal bars or mini-implants).<sup>7-12</sup> The recommended directions of initial pull have included vertical, buccal, and distal forces.<sup>8,9</sup> Such forces would also vary with the inclination of the impacted canine. Although the location of impaction has been widely investigated in clinical settings, studies of the relationship between the stresses generated by the orthodontic forces with the severity of impaction are not possible clinically.

For this reason, an engineering tool, the finite element (FE) modeling and analysis, provides the capability of simulating the effect of PIC traction under variable mechanical setups when the exact anatomy of jaws and teeth is reconstructed. The use of FE analysis in orthodontics has become a common research tool,<sup>13,14</sup> yet scarce in the investigation of PIC traction. Only 1

<sup>a</sup>Division of Orthodontics and Dentofacial Orthopedics, American University of Beirut Medical Center, Beirut, Lebanon.

<sup>b</sup>Department of Mechanical Engineering, Maroun Semaan Faculty of Engineering and Architecture, American University of Beirut, Beirut, Lebanon.

<sup>c</sup>Department of Industrial and Manufacturing Systems Engineering, College of Engineering and Computer Science, University of Michigan-Dearborn, Dearborn, Mich.

<sup>d</sup>Department of Orthodontics and Dentofacial Orthopedics, School of Dental Medicine, University of Pennsylvania, Philadelphia, Pa.

All authors have completed and submitted the ICMJE Form for Disclosure of Potential Conflicts of Interest, and none were reported.

Address correspondence to: Kinan G. Zeno, Division of Orthodontics and Dentofacial Orthopedics, American University of Beirut Medical Center, PO Box 11-0236, Riad El-Solh, Beirut 1107 2020, Lebanon; e-mail, [kz12@aub.edu.lb](mailto:kz12@aub.edu.lb) or [zenokinan@gmail.com](mailto:zenokinan@gmail.com).

Submitted, November 2018; revised and accepted, April 2019.

0889-5406/\$36.00

© 2019 by the American Association of Orthodontists. All rights reserved.

<https://doi.org/10.1016/j.ajodo.2019.04.035>

study exists in which stresses on the canine were examined in response to varied force angulations using a single simplified model.<sup>15</sup> Accordingly, we hypothesized that understanding and optimizing the mechanics delivered for PIC traction could be achieved through a comprehensive FE analysis applied to PIC locations and angulations accurately, located through 3D imaging from a number of patients. Accounting for individual variation in canine impaction, the FE modeling should help determine the optimal loading directions that yield the least stress on the PIC and therefore minimize potential side effects during treatment.

The aims of this study were to determine stress levels on the impacted canine when subjected to force activation in the buccal, vertical, and distal directions, and compare the generated stresses in relation to the severity of inclination of the impacted canine.

## MATERIAL AND METHODS

This study was approved by the Institutional Review Board at the American University of Beirut under IRB ID: OTO.JG.05. The material consisted of cone beam computed tomography (CBCT) scans of 21 patients (mean age 16.23 years) who had 30 PICs (12 with unilateral and 9 with bilateral PICs) and sought orthodontic treatment at our institution. The scans had been prescribed specifically for accurate localization of the impacted teeth after clinical examination and initial diagnostic panoramic or periapical radiograph. CBCT scans were selected according to the following criteria: PIC presence unilaterally or bilaterally, and good quality with sufficient field of view covering at least half of the maxilla in unilateral impaction and the entire maxillary arch in bilateral impaction.

Canines were considered to be at a higher potential for impaction when, at the recorded clinical examination, they were not palpable in the vestibule, prompting further radiographic confirmation, and when they had not erupted in the oral cavity beyond the age of 13 years (1 year after the normal maxillary permanent canine eruption age range of 11–12 years<sup>16</sup>). Exclusion criteria were the presence of a craniofacial anomaly or syndrome and any radiograph of limited field of view or of low resolution that did not allow accurate measurements.

The sample was subdivided into 2 severity subgroups on the basis of the inclination of the PIC to the virtually aligned canine (VAC), the simulated aligned tooth in its final posttreatment position in the arch measured on the reconstructed panoramic section of the CBCT scan<sup>2</sup> (Fig 1). Accordingly, the lower severity subgroup included canines with PIC/VAC  $\leq 30^\circ$  ( $17.9^\circ \pm 6.35^\circ$ ;  $n = 13$ ) and the higher severity subgroup comprised teeth with PIC/VAC  $> 30^\circ$ ; ( $45.7^\circ \pm 9.9^\circ$ ;  $n = 17$ ). The  $30^\circ$  cutoff

was chosen because it was close to the mean of the total sample ( $33.7^\circ \pm 16.3^\circ$ ), which coincidentally was an inclination about one third between a normally positioned canine and a horizontally impacted canine.

## Finite element modeling

A model was reconstructed from the CBCT scan (PaX-Zenith3D 2009.10; Vatech, Gyeonggi-do, Korea) of a female patient, aged 16 years 3 months, who presented with a maxillary left PIC. The scan, used to model anatomic components, consisted of 296 transversal sections with a 0.2 mm voxel resolution, and of the dimensions  $400 \times 400 \times 296$  mm. The CBCT images were saved in Digital Imaging and Communications in Medicine format and loaded into a 3D image-based modeling software Simpleware ScanIP (version 7.0; Synopsis, Exeter, UK). The model was segmented into bone and teeth using adaptive thresholding based on the gray scale value of those components in the scan. The periodontal ligament (PDL), not readily captured on the CBCT scan, was modeled by the duplication and expansion of the roots of all teeth by 1.5 voxel (0.3 mm) (Fig 2).

Individual variation was introduced by reproducing the impacted canine position from the CBCT scans in the prototype model. The global axes of the scans were redefined in all 21 scans to a unified fixed reference point prosthion (most anterior midsagittal point at the alveolar crest) (Fig 2). The 30 PIC 3D coordinates of the crown tip and apex were then measured in ScanIP. These measurements were used to determine the required repositioning of the PIC in the prototype model. The canine meshed stereolithography file was exported along with the prototype FE model to the +CAD module of ScanIP. A customized script was used in +CAD designed to automatically reposition the canine from the original position in the prototype model to the final position measured on the different CBCT scans (Fig 3). Within this script, a right PIC was reproduced as a mirror image of the left prototype canine.

After canine repositioning, bone was remodeled and a PDL layer was created for each of the 30 canines following the above-described steps of PDL modeling. Bone was adjusted to cover the entire root of the canine, thus eliminating any source of variation that was not related to position. The PIC crown was also cleared from any bony contact to allow for accurate detection of stresses on the PDL of the canine. A complete model was created, meshed, and then exported for each canine.

## Finite element analysis

The reconstructed model consisted of 639,455 tetrahedral elements and 126,476 nodes. Material properties

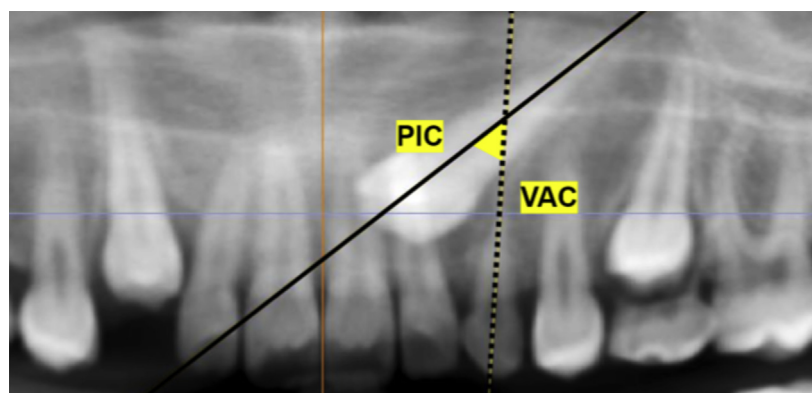


**Fig 1.** Illustration of angulation between PIC and the corresponding virtually aligned (VAC) position (dotted line), defining the angle PIC/VAC on a CBCT panoramic section. The VAC axis in this patient coincided with the axis of the retained primary canine.

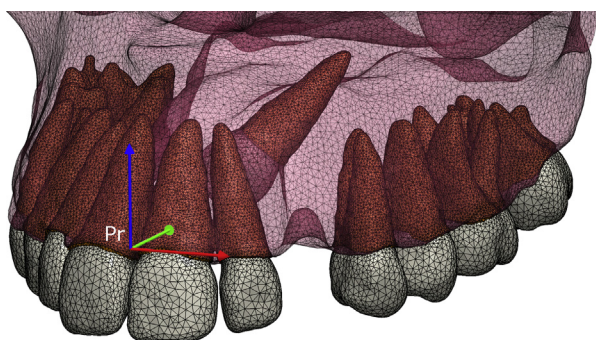


**Fig 2.** Anatomical reconstruction of the model meshed in ScanIP showing the teeth (white), PDL (orange), and alveolar bone (transparent pink). Global axis repositioned in all CBCT scans to point prosthion.

were defined for the anatomic components and appliances,<sup>15,17-20</sup> which were assumed to be homogeneous and isotropic materials (Table 1). A full constraint was applied on the maxilla (in translation and rotation) superiorly and posteriorly, representing the attachment to the zygomatic, palatal, and sphenoid bones. A traction force of 1.0 N was applied in 3 different force directions (Fig 4, A): a vertical extrusive force simulating the use of a ballista spring<sup>8</sup> or a palatal spring anchored over a transpalatal bar<sup>12</sup> or a mini-implant<sup>11</sup>; a distal force reproducing the pull toward a palatal bar or a palatal mini-implant; a buccal force reflecting the direct pull against the archwire.<sup>1</sup> The force was applied from the canine at a point on the archwire in the middle of the space defined for the alignment of the canine. The point of application of the force was at a button attachment placed in the center of the palatal surface of the PIC crown, simulating the clinical situation.

Von Mises stresses were recorded at the apical, middle, and cervical thirds of the PIC root, and for the whole root with each of the forces. Stresses in the PDL were averaged for each of the 3 levels of the canine root by randomly selecting and averaging the stress values at 300-400 elements around each region on the external surface of the PDL (Fig 4, B).

### Statistical analysis

A test of normality revealed that the data were normally distributed in both groups. A mixed between-within subjects 2-way ANOVA was used to test the effect of the between-subjects factor (severity) and the within-subjects factor (force direction) on the canine root stress. When a significant difference was detected, the Bonferroni post-hoc multiple comparison test was applied. *P* values <0.05 were considered statistically significant. The SPSS statistical software (version 20.0; IBM corporation, Armonk, NY) was employed to perform all statistical analyses.

### RESULTS

Distal and buccal forces resulted in higher stress ( $S = 6.64$  and  $6.41$  kPa, respectively) compared with the vertical force ( $S = 5.97$  kPa) (Table II). At the apical third of the PIC root, the stresses generated by different force directions were statistically significantly different ( $0.023 < P < 0.001$ ). The distal and vertical forces resulted in the highest ( $S = 7.73$  kPa) and least ( $S = 6.05$  kPa) stress, respectively. At the midroot area, stress amounts did not differ significantly between force directions. At the cervical level, the buccal force resulted in the highest stress ( $S = 7.21$  kPa) and the vertical force resulted in the least ( $S = 6.47$  kPa) stress. At the cervical

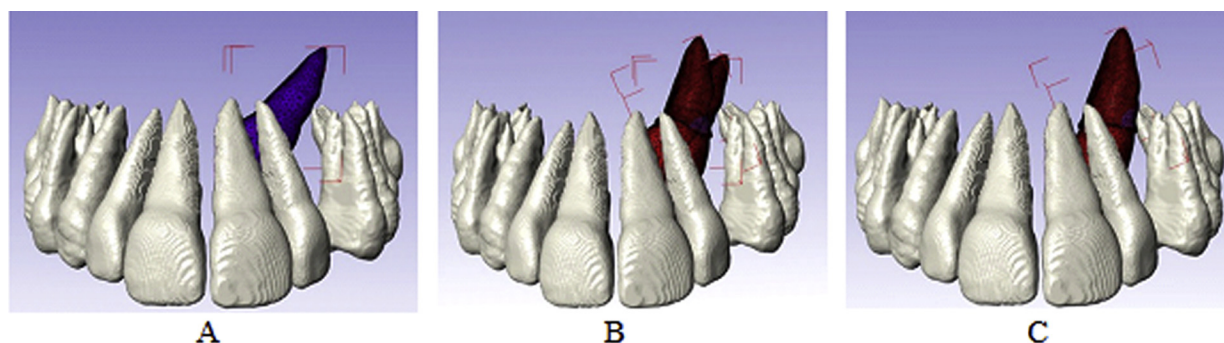


**Fig 3.** Canine repositioning. Copy of canine mesh inserted in arch (A) and repositioned to match position of apex and cusp tip of individual patient (B). Canine mesh repositioned and fixed (C).

**Table I.** Material properties used in the FE model

Material	Young's modulus ( $N/mm^2 = MPa$ )	Poisson's ratio
Tooth	20,000	0.20
PDL	0.68	0.45
Bone	15,750	0.33
Stainless steel	180,000	0.30

level and over the whole root, stress values were not statistically significantly different between buccal and distal forces but differed significantly between the vertical and distal forces ( $P = 0.027$  and  $P < 0.001$ , respectively), and between the vertical and buccal forces ( $P = 0.01$  and  $P = 0.02$ , respectively).

In the low-severity subgroup, the average stresses generated by the applied forces (buccal, distal, and vertical) differed significantly from each other in the apical region. Differences between vertical and distal forces as well as vertical and buccal forces were statistically significant at all root levels (Table III). The only statistically nonsignificant differences were for stresses at the middle, cervical, and whole root between buccal and distal forces. In all instances except at midroot, the stresses were highest with the distal force, followed by those from the buccal, and then the vertical forces.

In the higher severity subgroup, stresses generated by the vertical force were lower than and statistically significantly different from those generated by the buccal force at all levels except at midroot level (Table III). Stresses from the distal force were higher than those generated by the vertical force, but statistically significantly different only at the apical level and for the whole root. Differences between stress amounts in response to buccal and distal forces were significant in the middle and cervical regions, the distal force generating greater amounts at all but the cervical levels. This pattern of stress distribution was similar across severity groups

but different in amounts. The corresponding stress scales are illustrated in Figure 5.

## DISCUSSION

A new approach was introduced in this study of PIC traction that included a full 3D reconstruction of the maxillary arch and individual variations in PIC impaction severity. In contrast, prior research was based on the use of a simplified virtual array in a fragmented anatomic representation of jaw and teeth.<sup>16</sup> Accordingly, the results reflected the interaction of different load directions with a scale of impaction severity.

The distal followed by the buccal forces resulted in the highest stress over the root in general; the lowest stress was produced by the vertical load (Table II). Therefore, the distal and vertical forces generated the highest and least resistance to movement, respectively. This interpretation seemingly contradicts the engineering tenet that greater stress is consistent with greater strain within the PDL (stress [ $\sigma$ ] = strain [ $\epsilon$ ] x stiffness [ $E$ ]), thus greater initial movement. However, the interpretation is plausible in the context of the aberrant inclinations of the impacted canine within its bony housing. The clinical implication would be to apply a vertical force before or in conjunction with the distal force (Table II).

These considerations relate to the unique setting of PIC traction. In other orthodontic conditions, such as the distalization of posterior teeth or the retraction of canines into the first premolar extraction space, the teeth are not nearly as variable in their inclination and other positional characteristics as the PIC and are moved after initial alignment along a generally well defined track of an archwire unlike the traction of the PIC.

With the distal and buccal forces, stress at midroot was lower than that at the apical and cervical levels in

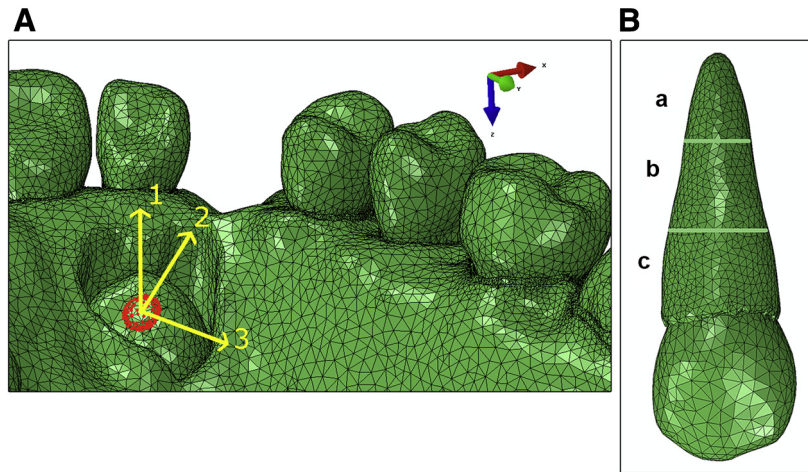


**Fig 4. A,** Forces (yellow arrows) applied on canines shown in vertical (1), buccal (2), and distal (3) directions. Forces were applied to a button attachment on the palatal surface of the canine (nodes highlighted in red). Model is shown from an oblique occlusal view. **B,** Element sets in which stresses were evaluated at different levels of the PIC root. Average stress was calculated for each third, the apical level (a), midroot level (b), cervical level (c), and the entire root by averaging all parts of the root.

**Table II.** Distribution of stress: Von Mises kPa mean ± (SD) according to direction of force at various levels of the canine root in the total group

Parameter	Buccal	Vertical	Distal	Pairwise comparisons (post-hoc) P		
				B vs V	B vs D	V vs D
Apical	6.92 (1.4)	6.05 (0.54)	7.73 (0.86)	0.008*	0.023*	<0.001*
Middle	5.10 (0.76)	5.39 (0.54)	5.21 (0.81)	0.384	0.990	0.990
Cervical	7.21 (0.93)	6.47 (0.63)	6.98 (0.65)	0.010*	0.750	0.027*
Average root	6.41 (0.78)	5.97 (0.35)	6.64 (0.57)	0.020*	0.390	<0.001*

\*Statistically significant:  $P < 0.05$ .

both severity groups, a finding that indicates tipping of the canine with the center of rotation in the middle third of the root (Fig 5). However, differential levels of stress between the distal and buccal forces were observed (Table III). Differences between apical/midroot and cervical/midroot stresses were greater with the buccal force in the high-severity group, probably related to the more horizontal direction of the impacted tooth. Similar stress differentials were observed with the distal force in the low-severity group, likely associated with the lower cusp tip location in this group, whereby a lower point of application of the distal force generates a greater moment of the force, thus the increased stresses (Fig 6).

The initial movement of the PIC and associated stress distribution on its root is determined by the relation between force direction and the canine's center of resistance (which is significantly affected by the surrounding alveolar bone). When the line of action of a vertical force

is the closest to the center of resistance, the resultant displacement would be mostly extrusion with minor tipping. However, the resultant tipping movement would be greater with the more severely inclined PIC. This association is reflected in the finding that within the higher severity group, the midroot stresses (5.13 kPa) were markedly lower than those at the apical (6.15 kPa) and cervical (6.71 kPa) levels, and within the less severe group, the stress at the midroot (5.73 kPa) was closer to that at the apical (5.94 kPa) and cervical (6.16 kPa) thirds (Fig 6; Table III).

**Clinical and research considerations**

Incorporating the anatomy of the entire maxilla with individual variation of the impacted canine yielded findings that are interpretable clinically and form the basis for future elaborate studies that would ultimately incorporate the FE model in actual treatment planning.

**Table III.** Comparison of stress distribution at various levels of the canine root in low- and high-severity subgroups: Von Mises kPa mean ± (SD)

Group	PIC/VAC < 30° = 13			Pairwise comparisons (post-hoc)			PIC/VAC > 30° = 17			Pairwise comparisons (post-hoc)		
	Buccal	Vertical	Distal	B/V	B/D	V/D	Buccal	Vertical	Distal	B/V	B/D	V/D
Apical	6.55 (0.78)	5.93 (0.23)	7.63 (0.94)	0.006*	0.002*	<0.001*	7.20 (1.67)	6.15 (0.68)	7.80 (0.81)	0.004*	0.180	<0.001*
Middle	5.26 (0.78)	5.73 <sup>+</sup> (0.46)	4.71 <sup>+</sup> (0.79)	0.001*	0.039	<0.001*	4.99 (0.75)	5.13 <sup>+</sup> (0.45)	5.59 <sup>+</sup> (0.60)	0.422	0.001*	0.013
Cervical	6.81 (0.58)	6.16 <sup>+</sup> (0.25)	7.16 (0.71)	<0.001*	0.096	<0.001*	7.51 (1.04)	6.71 <sup>+</sup> (0.73)	6.85 (0.59)	0.001*	0.004*	0.465
Average	6.21 (0.52)	5.94 (0.23)	6.50 (0.71)	0.014	0.093	0.004*	6.57 (0.92)	5.99 (0.42)	6.75 (0.42)	0.004*	0.401	<0.001*

+The only statistically significant differences between low- and high-severity groups were found at the middle root level with the vertical force (5.73 vs 5.13, respectively; *P* = 0.001) and the distal force (4.71 vs 5.59, respectively; *P* = 0.002) and at the cervical level with the vertical force (6.16 vs 6.71, respectively; *P* = 0.009).

\**P* value significant below 0.006.

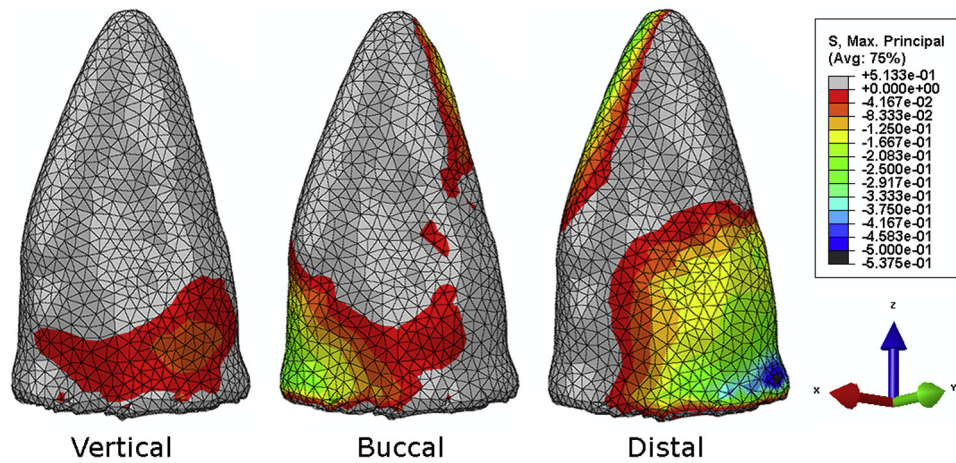


**Fig 5.** Simulation of stresses induced by a vertical force, yielding stresses mostly at the cervical root level; a buccal force, with stresses on the cervical to midlevel on the mesial surface, the apical level on the distal surface, and a cervical level on the palatal surface; and a distal force, with stresses mostly at the mid to apical level on the buccal surface. Note the location of the higher (blue) and lower (red) stresses. These illustrations relate to the simulation on a patient with a PIC/VAC angle of 53° (higher severity group); a similar general pattern of stress distribution was observed in the lower severity group.

To simulate the optimal condition of PIC traction, the arch was aligned, and sufficient space was provided for the canine. A force of 1.0 N was selected, also advocated by Han et al,<sup>21</sup> because it is in the middle range between 0.5 N and nearly 2.5 N applied in published studies or treatment reports.<sup>1,9,22,23</sup>

The significance of the average differences between the Von Mises stresses generated by the vertical and distal forces (0.6 kPa) and by the vertical and buccal forces (0.5 kPa) should be evaluated in association with the loading conditions. Given that a stress of 1 kPa is about 10.2 g/cm<sup>2</sup>, the equivalent forces to these differences would be 5 and 6 g/cm<sup>2</sup>, respectively. Because the average root surface of a maxillary canine is nearly 3 cm<sup>2</sup> (2.73 cm<sup>2</sup>),<sup>24</sup> the differences become

15 and 18 g, which correspond to nearly 15% and 20% of the originally applied force of 1.0 N (approximately 100 g), respectively. These percentages are large enough to be considered of clinical significance.

A single force applied to move the PIC within the dome-like structure of the maxilla includes more than one component. The direction of PIC traction should be determined according to the 3D position and inclination of the tooth, with prior planning of the prevailing force direction. The more stressful initial PIC traction at the cervical level under the buccal force in the more severe impactions (Table III) reflects more resistance to orthodontic traction. Accordingly, distal and vertical force directions would be preferable to buccal forces (at least) in the initial stages of canine traction,

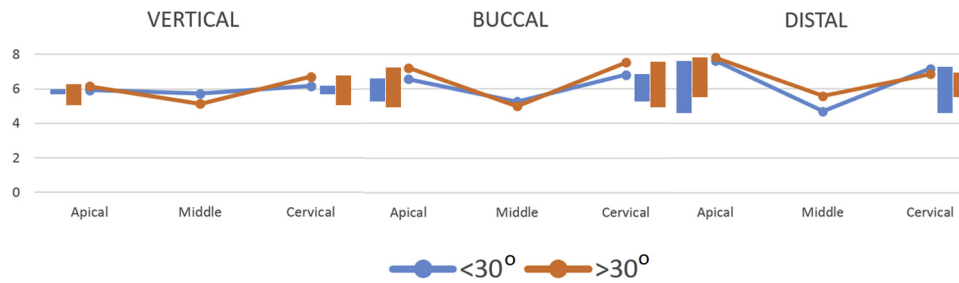


**Fig 6.** Graphic representation of differential in stress distribution (in kPa) at the apical, middle, and cervical root levels in the lower (*blue*) and higher (*orange*) severity groups. Stresses at midroot were the lowest with all force directions and across severity groups. The vertical bars represent the difference in Von Mises stresses between the apical and middle levels (on side of apical values) and between the cervical and middle levels (on side of cervical values). The greater stresses were generated by the buccal and distal forces. The differences between apical and cervical stresses relative to the midroot stresses were with the buccal force in the high-severity group and the distal force in the low-severity group.

particularly with more inclined canines, as they would move the tooth to a position where the buccal force would be less stressful in the final movement of the tooth within the arch. Published clinical observations support these conclusions.<sup>8,9</sup>

Moreover, the results suggest that the inclusion of a vertical component to either the buccal or the distal force at the indicated time of treatment (depending on the PIC inclination) could reduce stress-point concentration, thus generating more even stress distribution over the root and alleviating apical stress concentration.

The concordance of clinical observations with the study outcomes supports the application of finite element modeling, although the construction of the FE model is based on assumptions related to material properties. The remarkably time-consuming process of generating the FE model limited the ability to include a larger sample and develop an original replica for each patient, requiring the precise translation of PIC variations from the CBCT positional coordinates instead. Nonreproduced differences in tooth and arch sizes may have affected the outcome, but the general trend of results is expected to hold. In contrast, not varying those measures provided a control for the unrepresented variations.

This study was limited to evaluating the initial response to a force. Deeper understanding of the PIC displacement would require the application of a dynamic time-dependent motion analysis through FE. Also, this study did not investigate different force magnitudes; however, the outcome of linear material properties probably would have been similar because the response to the force would have been proportional. Force variation

would make a difference when nonlinear material properties are developed.

## CONCLUSIONS

1. The inclusion of individual variations to FE modeling of PIC traction helped determine response patterns that reflected the importance of implementing personalized rather than generic treatment approaches.
2. Stress varied with force directions, the distal and buccal forces yielding higher stress values than the vertical force. Stresses were distributed differentially at the various levels of the canine root and were lowest at the middle level with all force directions and in both severity groups, reflecting the initial generated tipping movement.
3. The higher stresses generated by the buccal force at the cervical level with the more severely inclined canines indicate more resistance to movement and would suggest the application of distal and/or vertical force in the initial stages of canine traction. A direct buccal force would be applied when the impacted canine is closer to the alveolar crest.

## ACKNOWLEDGMENTS

This article was funded by Intramural research funds from the American University of Beirut Faculty of Medicine (Tabourian Dentofacial Educational Fund, Division of Orthodontics and Dentofacial Orthopedics) and Maroun Semaan Faculty of Engineering and Architecture.

## REFERENCES

1. Bishara SE. Clinical management of impacted maxillary canines. *Semin Orthod* 1998;4:87-98.
2. Zeno KG, Ghafari JG. Palatally impacted canines: a new 3-dimensional assessment of severity based on treatment objective. *Am J Orthod Dentofacial Orthop* 2018;153:387-95.
3. Becker A, Chaushu G, Chaushu S. Analysis of failure in the treatment of impacted maxillary canines. *Am J Orthod Dentofacial Orthop* 2010;137:743-54.
4. Manne R, Gandikota C, Juvvadi SR, Rama HR, Anche S. Impacted canines: etiology, diagnosis, and orthodontic management. *J Pharm Bioallied Sci* 2012;4(Suppl 2):S234-8.
5. Litsas G, Acar A. A review of early displaced maxillary canines: etiology, diagnosis and interceptive treatment. *Open Dent J* 2011;5:39-47.
6. Ericson S, Kuroi PJ. Resorption of incisors after ectopic eruption of maxillary canines: a CT study. *Angle Orthod* 2000;70:415-23.
7. Becker A, Zilberman Y. The palatally impacted canine: a new approach to treatment. *Am J Orthod* 1978;74:422-9.
8. Jacoby H. The "ballista spring" system for impacted teeth. *Am J Orthod* 1979;75:143-51.
9. Kornhauser S, Abed Y, Harari D, Becker A. The resolution of palatally impacted canines using palatal-occlusal force from a buccal auxiliary. *Am J Orthod Dentofacial Orthop* 1996;110:528-34.
10. Bowman SJ, Carano A. The Kilroy spring for impacted teeth. *J Clin Orthod* 2003;37:683-8.
11. Haydar SG, Uçkan S, Sesen C. A method for eruption of impacted teeth. *J Clin Orthod* 2003;37:430-3.
12. Tepedino M, Chimenti C, Masedu F, Potrubacz MI. Predictable method to deliver physiologic force for extrusion of palatally impacted maxillary canines. *Am J Orthod Dentofacial Orthop* 2018;153:195-203.
13. Holberg C, Winterhalder P, Holberg N, Wichelhaus A, Rudzki-Janson I. Indirect miniscrew anchorage: biomechanical loading of the dental anchorage during mandibular molar protraction-an FEM analysis. *J Orofac Orthop* 2014;75:16-24.
14. Suzuki A, Masuda T, Takahashi I, Deguchi T, Suzuki O, Takano-Yamamoto T. Changes in stress distribution of orthodontic miniscrews and surrounding bone evaluated by 3-dimensional finite element analysis. *Am J Orthod Dentofacial Orthop* 2011;140:e273-80.
15. Zhang J, Wang XX, Ma SL, Ru J, Ren XS. 3-dimensional finite element analysis of periodontal stress distribution when impacted teeth are tracted. *Hua Xi Kou Qiang Yi Xue Za Zhi* 2008;26:19-22.
16. Moorrees CFA, Grøn AM, Le Bret LML, Yen PKJ, Fröhlich FJ. Growth studies of the dentition: a review. *Am J Orthod* 1969;55:600-16.
17. Bourauel C, Freudenreich D, Vollmer D, Kobe D, Drescher D, Jäger A. Simulation of orthodontic tooth movements. A comparison of numerical models. *J Orofac Orthop* 1999;60:136-51.
18. Field C, Ichim I, Swain MV, Chan E, Darendeliler MA, Li W, et al. Mechanical responses to orthodontic loading: a 3-dimensional finite element multi-tooth model. *Am J Orthod Dentofacial Orthop* 2009;135:174-81.
19. Tanne K, Sakuda M, Burstone CJ. Three-dimensional finite element analysis for stress in the periodontal tissue by orthodontic forces. *Am J Orthod Dentofacial Orthop* 1987;92:499-505.
20. Kojima Y, Fukui H. Numerical simulations of canine retraction with T-loop springs based on the updated moment-to-force ratio. *Eur J Orthod* 2012;34:10-8.
21. Han G, Huang S, Von den Hoff JW, Zeng X, Kuijpers-Jagtman AM. Root resorption after orthodontic intrusion and extrusion: an intraindividual study. *Angle Orthod* 2005;75:912-8.
22. Yadav S, Chen J, Upadhyay M, Jiang F, Roberts WE. Comparison of the force systems of 3 appliances on palatally impacted canines. *Am J Orthod Dentofacial Orthop* 2011;139:206-13.
23. Reitan K. Effects of force magnitude and direction of tooth movement on different alveolar bone types. *Angle Orthod* 1964;34:244-55.
24. Jepsen A. Root surface measurement and a method for x-ray determination of root surface area. *Acta odontol scand* 1963;21:35-46.